

Evaluation of Seismic Slope Displacements Based on Fully Coupled Sliding Mass Analysis and NGA-West2 Database

Wenqi Du¹; Gang Wang, M.ASCE²; and Duruo Huang³

Abstract: In this study, two predictive models for seismic slope displacements are developed based on an equivalent-linear fully coupled sliding mass model and 3,714 ground-motion recordings selected from the Next Generation Attenuation (NGA)-West2 database. Both predictive models use the sliding system's yield acceleration and initial fundamental period T_s as predictor variables, whereas they use different sets of vector intensity measures (i.e., spectral acceleration at a degraded period of the system $1.5T_s$ and Arias intensity in one model; peak ground acceleration and spectral acceleration at 2 s in another). The models are developed following the framework of model BT07, a predictive model for estimating the sliding displacement based on the fully coupled sliding mass analysis. The framework consists of two parts, namely, the probability of "zero" displacement (<1 cm) and the statistical distribution of "nonzero" displacement (≥ 1 cm). The proposed models in this study can be regarded as updates of the BT07 model, which can be used for estimating earthquake-induced displacements for a wide range of slope cases. DOI: [10.1061/\(ASCE\)GT.1943-5606.0001923](https://doi.org/10.1061/(ASCE)GT.1943-5606.0001923). © 2018 American Society of Civil Engineers.

Author keywords: Seismic sliding displacement; Fully coupled analysis; Predictive models; Next Generation Attenuation (NGA)-West2 database.

Introduction

Estimating earthquake-induced displacement of slopes is an important topic for evaluating and mitigating seismic hazards (Jibson 2011). Since Newmark's (1965) pioneering work on the rigid sliding block model, many researchers (e.g., Saygili and Rathje 2008; Du and Wang 2016) have proposed empirical equations to predict the sliding displacement, which is regarded as a quantitative index in various applications (e.g., Du and Wang 2014; Rathje et al. 2014). Yet, the Newmark model is most suitable for modeling shallow landslides of stiff materials that move along a well-defined slip surface. Flexible/deep sliding masses generally deform internally when subjected to seismic shaking. Therefore, the dynamic behavior of the sliding mass should be considered in the analysis. For this purpose, Rathje and Bray (2000) proposed a fully coupled sliding mass model to simulate stick-slip and deformation of the flexible mass simultaneously.

Bray and Travararou (2007) were the first to develop a predictive model for estimating the sliding displacement D based on the fully coupled sliding mass analysis. The model (called BT07 hereafter) predicts D as a function of yield acceleration (k_y), initial fundamental period T_s of the slope, and the spectral acceleration of the ground motion at a degraded period $1.5T_s$ [$S_a(1.5T_s)$]. The moment magnitude (M_w) of the earthquake is also included in the model to correct prediction bias. Detailed information of the existing predictive models is summarized in Table 1.

¹Senior Research Fellow, Institute of Catastrophe Risk Management, Nanyang Technological Univ., 50 Nanyang Ave., Singapore 639798.

²Associate Professor, Dept. of Civil and Environmental Engineering, Hong Kong Univ. of Science and Technology, Clear Water Bay, Hong Kong (corresponding author). Email: gwang@ust.hk

³Assistant Professor, Dept. of Hydraulic Engineering, Tsinghua Univ., Beijing 100084, China.

Note. This manuscript was submitted on April 30, 2017; approved on February 21, 2018; published online on May 31, 2018. Discussion period open until October 31, 2018; separate discussions must be submitted for individual papers. This technical note is part of the *Journal of Geotechnical and Geoenvironmental Engineering*, © ASCE, ISSN 1090-0241.

Recent development of the Next Generation Attenuation (NGA)-West2 database (Ancheta et al. 2014) provides an opportunity to update these predictive models based on an extended ground-motion database. Therefore, this paper develops two predictive models for seismic slope displacements based on the fully coupled sliding mass analysis and 3,714 ground-motion recordings selected from the NGA-West2 database. The predictive models follow a similar analysis framework of Bray and Travararou (2007) using two sets of vector intensity measures (IMs) as predictor variables. They can be regarded as updates of the BT07 model.

Seismic Slope Displacement Analysis

Ground Motion Database

A subset of the Pacific Earthquake Engineering Research (PEER) Center's NGA-West2 database is adopted for calculating the seismic slope displacements based on the fully coupled sliding mass analysis. The ground-motion selection criteria introduced by Campbell and Bozorgnia (2014) are used to exclude some low-quality recordings. To avoid any bias caused by low-amplitude motions, we further exclude ground motions that fail to satisfy the following criteria: (1) $M_w \geq 4.5$, (2) rupture distance (R_{rup}) ≤ 200 km, and (3) peak ground acceleration (PGA) $\geq 0.01g$. The final database consists of 3,714 recordings from 102 earthquakes. The M_w - R_{rup} distribution of the selected ground motions is shown in Fig. 1. The two horizontal components of each recording are regarded as independent records. For each acceleration-time series, the maximum value computed from both the positive and the negative directions is taken as the displacement D for this record.

Fully Coupled Sliding Mass Analysis

The fully coupled sliding mass analysis follows Rathje and Bray (2000). The sliding mass is simplified as a generalized single-degree-of-freedom system governed by its first mode of vibration. The nonlinear responses of the soil are modeled using an

Table 1. Summary of existing predictive models based on fully coupled approach

| Predictor variables | Earthquake category | Number of earthquakes | Number of records | Reference |
|-----------------------------------|---------------------|-----------------------|-------------------|---------------------------------|
| $k_y, T_s, S_a(1.5T_s), M_w$ | Shallow crustal | 41 | 688 | Bray and Travararou (2007) |
| $k_y, T_s, S_a(2.0T_s), PGV$ | Near-fault | 46 | 243 | Song and Rodriguez-Marek (2015) |
| $k_y, T_s, S_a(1.5T_s), M_w$ | Subduction | — | 2,244 | Macedo et al. (2017) |
| $k_y, T_s, S_a(1.5T_s), I_a, M_w$ | Shallow crustal | 102 | 3,714 | This study |
| $k_y, T_s, PGA, S_a(2 s)$ | | | | |

Note: $S_a(1.5T_s), S_a(2.0T_s)$ = spectral acceleration at a degraded period $1.5T_s$ and $2.0T_s$, respectively; PGV = peak ground velocity; and $S_a(2 s)$ = spectral acceleration at 2 s.

equivalent-linear approach, and permanent displacement would occur if base acceleration exceeds k_y (cf. Wang 2012).

The sliding mass was assigned with a constant unit weight of 18 kN/m³ and a plasticity index of 30. The shear modulus reduction and material damping ratio curves proposed by Darendeli (2001) were used to model the nonlinear properties of soils; the input parameters for the Darendeli model were assigned as follows: overconsolidation ratio (OCR) is 1, loading frequency (f) is 1 Hz, number of cycles (N) is 10, and the mean confining pressure is 101 kPa (1 atm).

The variables T_s and k_y are commonly used to characterize the dynamic stiffness and strength of an earth slope. In this study, the earthquake-induced displacements were computed for slopes with specified combinations of T_s (0–2 s) and k_y (0.01–0.5g). Here, T_s can be estimated by $T_s = 4H/V_s$, where H and V_s are the average height and shear-wave velocity of a sliding mass, respectively. For nonzero T_s , H varied between 5 and 100 m, and V_s varied between 200 and 400 m/s. The model reduces to the original Newmark's model for the rigid slope case ($T_s = 0$).

Selection of Predictor Variables

When developing a new model, it is important to identify the optimal IMs as predictor variables. Specifically, a set of IMs used in engineering applications should satisfy the efficiency and sufficiency criteria (Luco and Cornell 2007). Efficiency requires the model has small variability in the prediction; sufficiency requires that the model would not significantly depend on other seismological parameters such as magnitude and distance of the earthquake.

Several ground-motion IMs were used to examine their correlations with D . These IMs include PGA, Arias intensity (I_a), spectral acceleration (S_a) at various periods, and T_s -dependent S_a ordinates [e.g., $S_a(1.5T_s)$], etc. For each (T_s, k_y) case, nonlinear regression analysis was performed by fitting a quadratic form for a

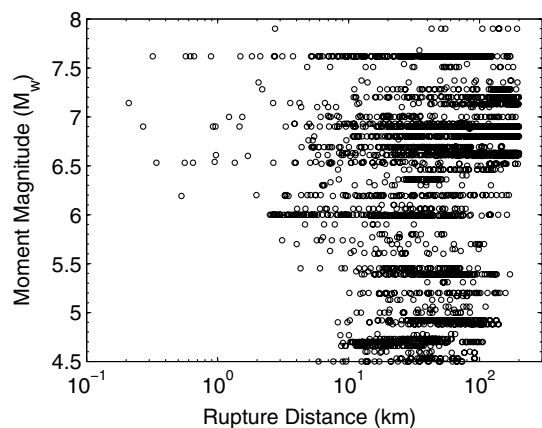


Fig. 1. Distribution of moment magnitude versus rupture distance for recordings selected from the NGA-West2 database.

scalar IM or a vector IM. The calculated standard errors for various slope conditions using the selected scalar and vector IMs are illustrated in Figs. S1 and S2 in the Supplemental Data, respectively. The results indicate that using the [$S_a(1.5T_s), I_a$] vector is an ideal choice to optimize the overall efficiency of the model. Another option is to use the [PGA, $S_a(2 s)$] vector, which also provides reasonably good efficiency in regressing D .

Proposed Models

Most of the existing models have adopted the mixed-random variable approach, which consists of estimating the probability of negligible “zero” displacement and developing the conditional probability density function of nonzero displacement. In this study, displacements smaller than 1 cm are regarded as “zero” displacement following Bray and Travararou (2007). Such truncation is necessary to avoid prediction biases caused by small displacements that have little engineering significance. Yet, an inappropriate choice of the truncation may affect the distribution of residuals. Several values were tested, and the truncation of 1 cm was found to best preserve the normality of the residuals.

Two sets of functional forms using different IMs as predictors are then proposed following the mixed-random variable model. Each predictive model was developed in two steps: (1) predicting the probability of negligible “zero” displacement ($D < 1$ cm), and (2) estimating the distribution (median and standard deviation) of nonzero displacement ($D \geq 1$ cm). A probit regression analysis (Bray and Travararou 2007) was used to derive the probability of zero displacement, while the nonzero displacements were analyzed using the nonlinear mixed-effects regression analysis.

[$S_a(1.5T_s), I_a$] Model

The probability function of “zero” displacement is derived as

$$P(D = 0) = 1 - \Phi \left(\frac{-2.282 - 2.459 \ln(k_y) - 0.744T_s \ln(k_y)}{-2.057T_s + 1.906 \ln S_a(1.5T_s) + 0.57 \ln I_a} \right) \quad (1)$$

where $P(D = 0)$ = estimated probability of zero displacement ($D < 1$ cm); Φ = standard normal cumulative distribution function; $S_a(1.5T_s)$ = spectral acceleration at $1.5T_s$ (g); and I_a = Arias intensity (m/s).

Fig. 2 shows the predicted zero probabilities associated with the empirical data selected from the present data set versus $S_a(1.5T_s)$, k_y , and T_s , respectively. The proposed model generally captures the trends of zero displacement. The zero probability increases as $S_a(1.5T_s)$ decreases or k_y increases; with respect to T_s , the lowest zero probability occurs at T_s in the range of 0.2–0.4 s, possibly due to the resonance effect.

The median nonzero displacement can be estimated by nonlinear mixed-effects regression analysis using the nonzero displacement data ($D \geq 1$ cm) as

$$\begin{aligned} \ln D = & -4.047 - 2.522 \ln(k_y) - 0.234(\ln(k_y))^2 + 0.506T_s \\ & - 0.651T_s^2 - 0.286T_s \ln(k_y) + 1.709 \ln S_a(1.5T_s) \\ & + 0.204 \ln(k_y) \ln S_a(1.5T_s) - 0.842\max(\ln S_a(1.5T_s), 0) \\ & + 0.352M_w + 0.486 \ln I_a + \varepsilon \end{aligned} \quad (2)$$

where D = nonzero displacement in centimeters; and ε = normally distributed (total) residuals with zero mean and standard deviation $\sigma_{\ln D}$. All the coefficients yield very small p -values (commonly used in statistical hypothesis testing), so they are statistically significant. Note that Eq. (2) is only applicable to $T_s \geq 0.05$ s,

because this functional form exhibits an underprediction bias when $T_s = 0$ s. Therefore, for rigid slope cases of $T_s < 0.05$ s, the function form for the median nonzero displacement is rewritten as

$$\begin{aligned} \ln D = & -3.707 - 2.522 \ln(k_y) - 0.234(\ln(k_y))^2 + 1.709 \ln \text{PGA} \\ & + 0.204 \ln(k_y) \ln \text{PGA} - 0.842\max(\ln \text{PGA}, 0) \\ & + 0.352M_w + 0.486 \ln I_a + \varepsilon \end{aligned} \quad (3)$$

Note that $S_a(1.5T_s)$ is replaced by PGA in Eq. (3) for practical use.

Fig. 3 shows the total residuals of Eqs. (2) and (3) with respect to k_y , T_s , $S_a(1.5T_s)$, I_a , and M_w , respectively. In each plot, the residuals are partitioned into several bins; the open square symbol denotes the local mean of residuals in each bin. In general, no clear

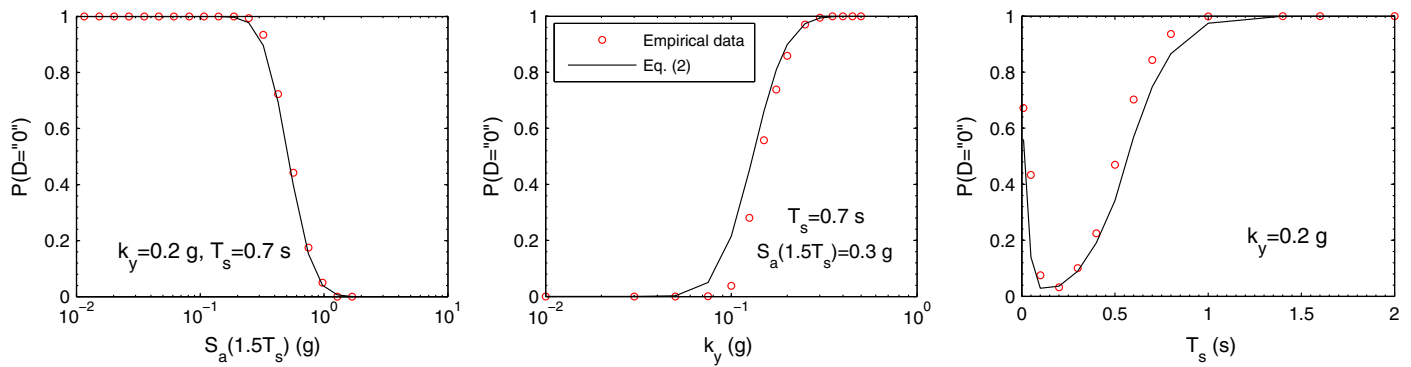


Fig. 2. Predicted probabilities of zero displacement for the $[S_a(1.5T_s), I_a]$ model compared with empirical data versus $S_a(1.5T_s)$, k_y , and T_s , respectively.

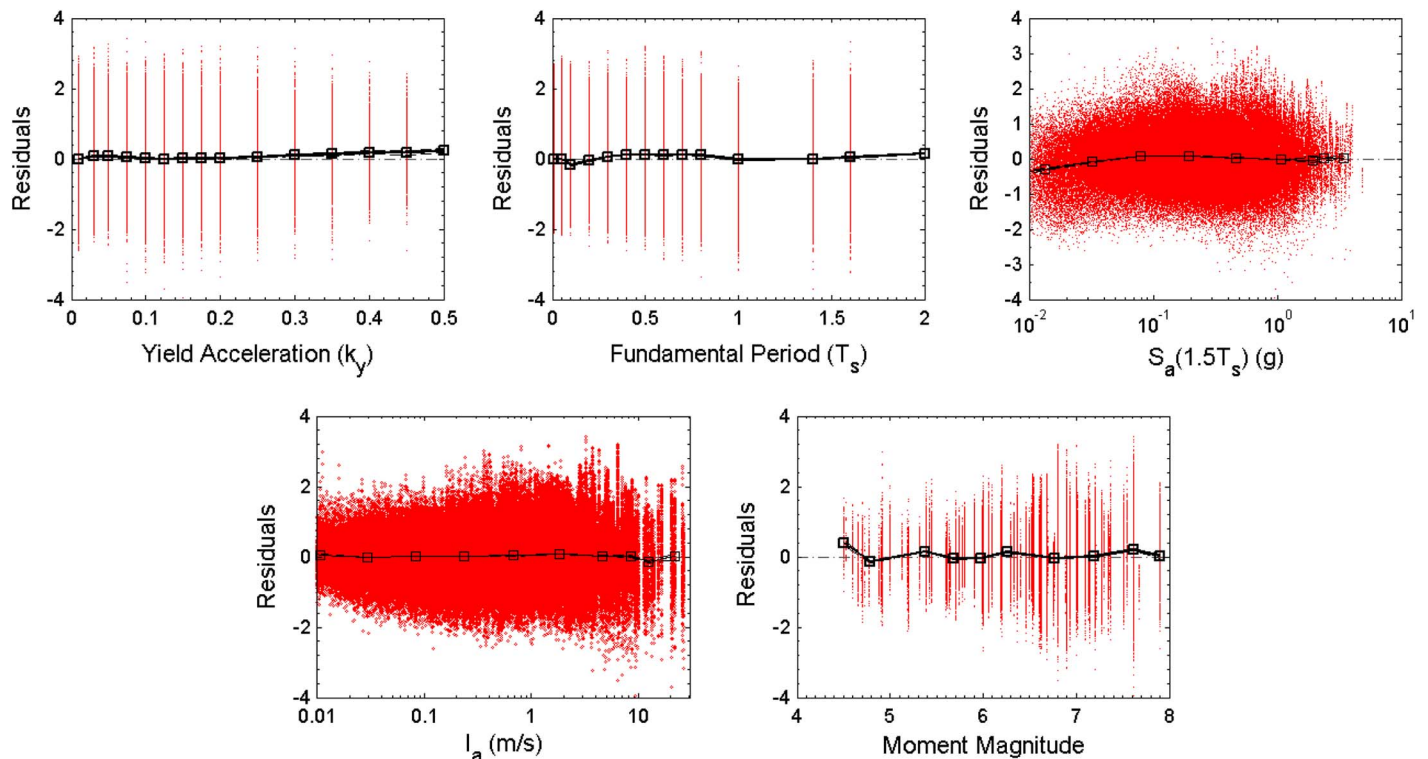


Fig. 3. Distribution of residuals for the $[S_a(1.5T_s), I_a]$ model with respect to predictor variables.

Table 2. Variability coefficients of proposed models

| Model | τ | σ | $\sigma_{\ln D}$ |
|--------------------------|--------|----------|------------------|
| $[S_a(1.5T_s), I_a]$ | 0.26 | 0.64 | 0.69 |
| $[PGA, S_a(2\text{ s})]$ | 0.21 | 0.71 | 0.74 |

Note: $S_a(1.5T_s)$ = spectral acceleration at a degraded period $1.5T_s$; $S_a(2\text{ s})$ = spectral acceleration at 2 s; and τ , σ , and $\sigma_{\ln D}$ = standard deviations of between-event, within-event, and total residuals, respectively.

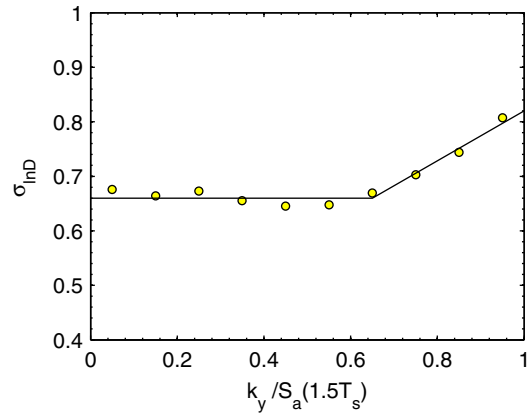
biases with respect to these predictor variables can be observed. There are some biased local means [e.g., $S_a(1.5T_s) < 0.05g$], which is not a critical issue since the displacements for these cases are less significant.

The variability coefficients of the proposed model are listed in Table 2, and $\sigma_{\ln D}$ obtained from the mixed-effects regression is 0.69. It is tempting to examine the relationship between $\sigma_{\ln D}$ and $k_y/S_a(1.5T_s)$ values, which is shown in Fig. 4. The standard deviations become larger for larger $k_y/S_a(1.5T_s)$ bins, so a bilinear relationship is proposed as

$$\sigma_{\ln D} = \begin{cases} 0.66 & \text{for } \frac{k_y}{S_a(1.5T_s)} < 0.65 \\ 0.36 + 0.46 \cdot \frac{k_y}{S_a(1.5T_s)} & \text{for } \frac{k_y}{S_a(1.5T_s)} \geq 0.65 \end{cases} \quad (4)$$

As demonstrated in Fig. 4, the bilinear model appropriately fits the empirical points.

In summary, the probability of zero displacement is specified via Eq. (1); the nonzero displacement is assumed to follow a lognormal distribution with median displacement D provided in Eqs. (2) and (3) and $\sigma_{\ln D}$ specified in Eq. (4). The probability of seismic displacement exceeding a given displacement value d can be estimated as

**Fig. 4.** Calculated binned standard deviations versus $k_y/S_a(1.5T_s)$ for the $[S_a(1.5T_s), I_a]$ model.

$$P(D > d) = [1 - P(D = 0)] \cdot \left[1 - \Phi \left(\frac{\ln d - \ln D}{\sigma_{\ln D}} \right) \right] \quad (5)$$

The predicted displacement according to a specified percentile p (in decimal form) can then be estimated as

$$\ln D_p = \ln \bar{D} + \sigma_{\ln D} \cdot \Phi^{-1} \left(\frac{p - P(D = 0)}{1 - P(D = 0)} \right) \quad (6)$$

where Φ^{-1} = inverse standard normal cumulative distribution function.

[PGA, $S_a(2\text{ s})$] Model

Using PGA and $S_a(2\text{ s})$ as predictors, the probability of zero displacement can be evaluated as

For $T_s \leq 0.2\text{ s}$

$$P(D = 0) = 1 - \Phi \left(\begin{array}{l} -1.521 - 3.783 \ln k_y - 0.152(\ln k_y)^2 + 18.26T_s - 36.30T_s^2 \\ + 3.255 \ln \text{PGA} + 0.533 \ln(S_a(2s)) \end{array} \right) \quad (7a)$$

For $T_s \geq 0.3\text{ s}$

$$P(D = 0) = 1 - \Phi \left(\begin{array}{l} -1.00 - 3.837 \ln k_y - 0.299(\ln k_y)^2 - 3.423T_s + 0.77T_s^2 \\ + 0.804 \ln \text{PGA} + 1.145 \ln(S_a(2s)) - 0.491 \ln T_s \ln(\text{PGA}/k_y) \end{array} \right) \quad (7b)$$

where k_y , T_s , PGA, $S_a(2\text{ s})$, and Φ are as defined previously. A notable feature of this model is that it calculates the probability of zero displacement for short periods ($T_s \leq 0.2\text{ s}$) and moderate-to-long periods ($T_s \geq 0.3\text{ s}$) separately. Linear interpolation can be used for obtaining the zero probability for T_s between 0.2 and 0.3 s. This two-part statistical analysis allows more flexibility in capturing the zero probability versus T_s . Fig. 5 shows the predicted zero probabilities via Eq. (7) compared with the empirical data with respect to k_y and T_s , respectively. The predictive curves are in reasonable agreement with empirical data.

The functional form of the predicted median nonzero displacement is written as follows:

$$\begin{aligned} \ln D = & b_0(k_y, T_s) - 2.209 \ln(k_y) - 0.141(\ln(k_y))^2 \\ & + (1.414 + 0.359 \ln(k_y)) \ln \text{PGA} - 0.135(\ln \text{PGA})^2 \\ & - 0.294T_s \ln(k_y) + (0.653 - 0.307 \ln(k_y)) \ln S_a(2s) \\ & + 0.135(\ln S_a(2s))^2 + \varepsilon \end{aligned} \quad (8)$$

where $b_0(k_y, T_s)$ is a piecewise function as

$$b_0(k_y, T_s) = \begin{cases} 0.641 - 1.257T_s \ln k_y & \text{if } T_s \leq 0.05 \text{ s} \\ 1.818 + 0.073 \ln k_y + (0.393 + 0.045 \ln k_y) \ln(T_s) & \text{if } 0.05 \text{ s} < T_s \leq 0.2 \text{ s} \\ 0.979 - 0.128 \ln(T_s) & \text{if } 0.2 \text{ s} < T_s \leq 0.4 \text{ s} \\ 0.231 - 0.944 \ln(T_s) & \text{if } 0.4 \text{ s} < T_s \leq 0.8 \text{ s} \\ -0.064 - 2.267 \ln(T_s) & \text{if } 0.8 \text{ s} < T_s \leq 1.4 \text{ s} \\ 0.331 - 3.442 \ln(T_s) & \text{if } T_s > 1.4 \text{ s} \end{cases} \quad (9)$$

Eq. (8) includes a quadratic function of $\ln(\text{PGA})$ and $\ln[S_a(2s)]$ and a piecewise function $b_0(k_y, T_s)$. All coefficients in Eqs. (8) and (9) are statistically significant.

Fig. 6 illustrates the total residuals with respect to k_y , T_s , PGA, $S_a(2s)$, and M_w , respectively. Again, the residuals are partitioned into several bins, and the local means are shown in each plot.

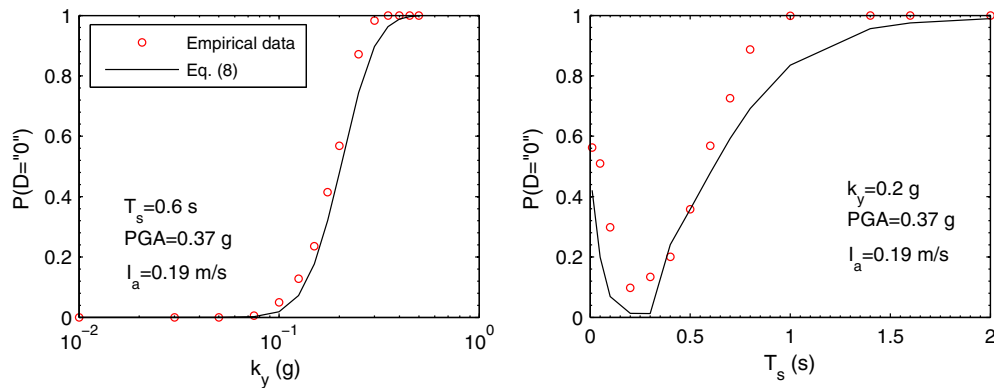


Fig. 5. Predicted probabilities of zero displacement for the [PGA, $S_a(2s)$] model compared with empirical data versus k_y and T_s , respectively.

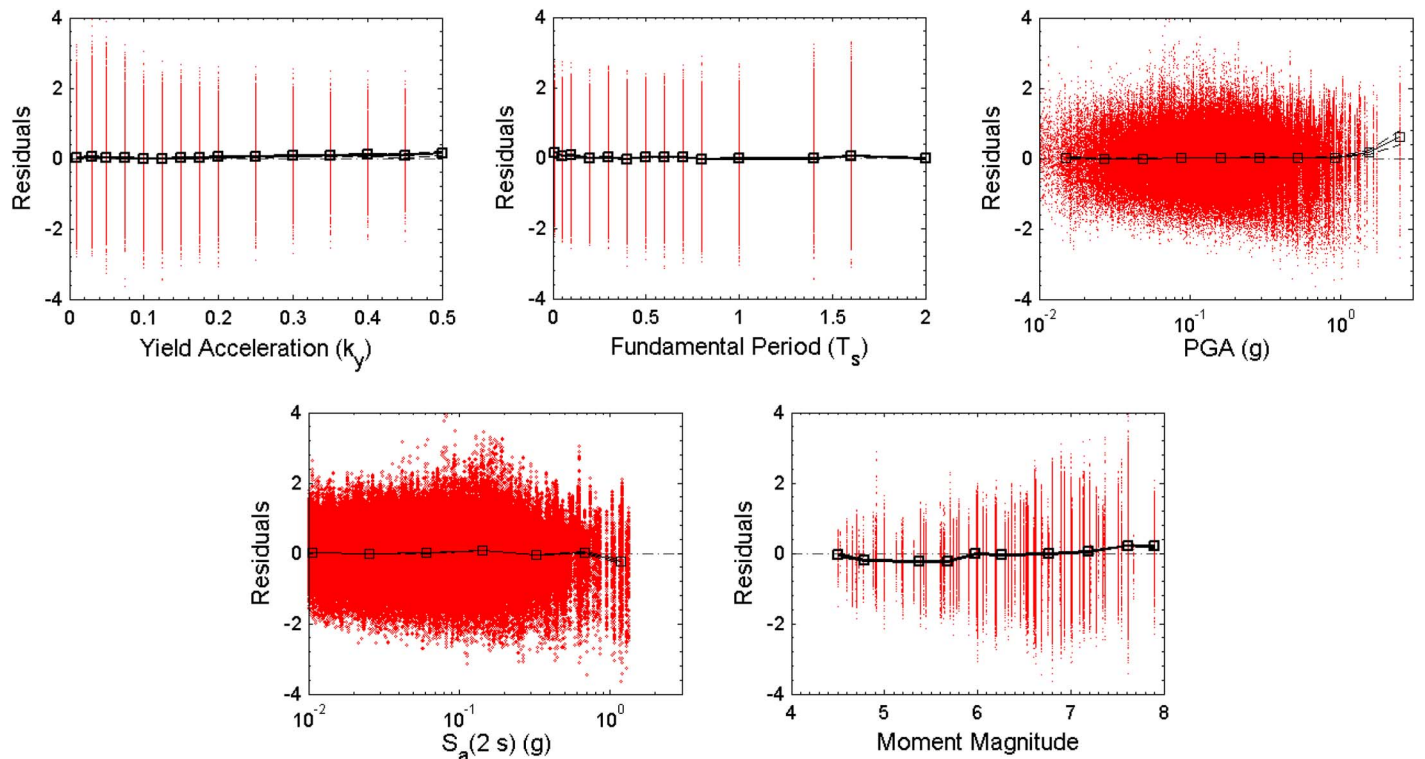


Fig. 6. Distribution of total residuals for the [PGA, $S_a(2s)$] model with respect to predictor variables.

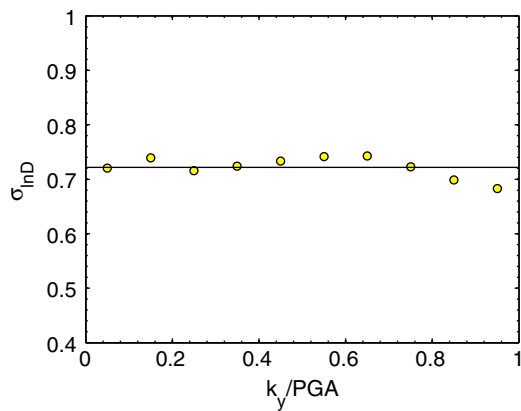


Fig. 7. Calculated binned standard deviations versus k_y/PGA for the $[PGA, S_a(2\text{ s})]$ model.

The residuals are generally unbiased with respect to the predictor variables used. Specifically, the residuals versus M_w are only slightly biased, implying that the $[PGA, S_a(2\text{ s})]$ model can satisfy the sufficiency requirement.

As listed in Table 2, the standard deviation of the total residuals based on Eqs. (8) and (9) is 0.74. Fig. 7 shows the computed $\sigma_{\ln D}$ for bins of k_y/PGA values. The $\sigma_{\ln D}$ values do not show a clear dependence on k_y/PGA , and thus an average $\sigma_{\ln D}$ value (0.72) can be used for all cases.

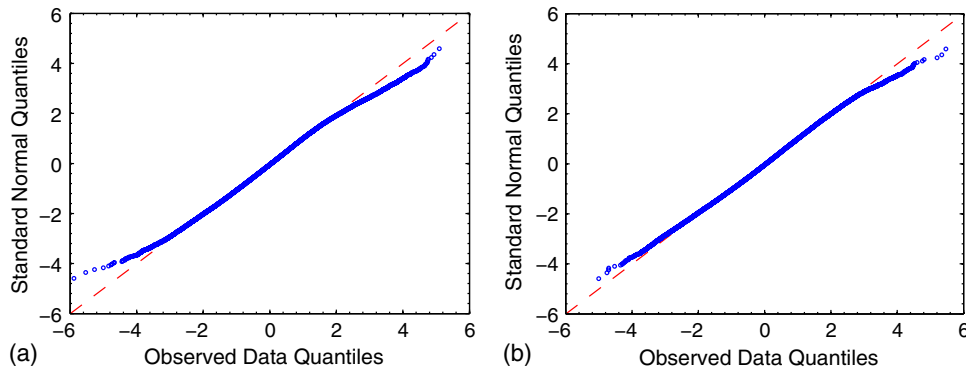


Fig. 8. Q-Q plots of the displacement residuals: (a) the $[S_a(1.5T_s), I_a]$ model; and (b) the $[PGA, S_a(2\text{ s})]$ model.

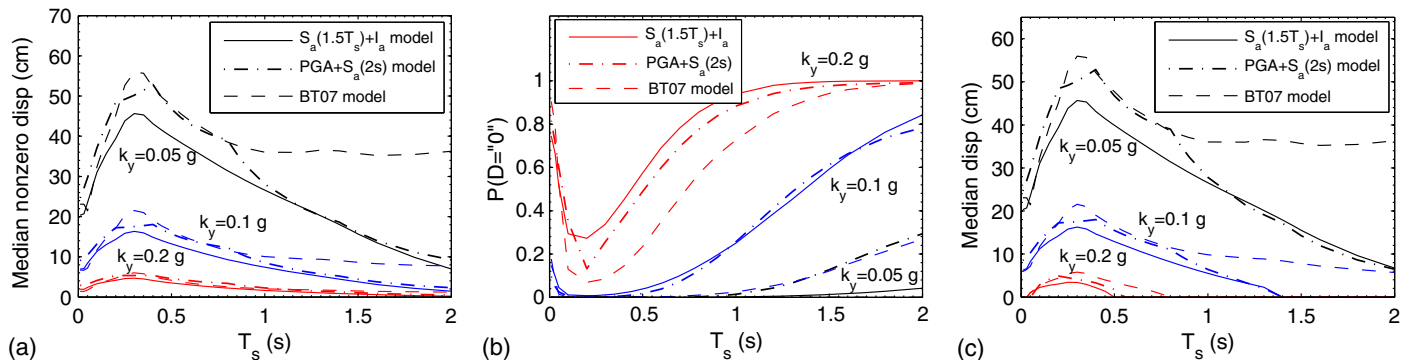


Fig. 9. Comparisons of the predictions of three models: (a) predicted median nonzero displacements; (b) probability of zero displacements; and (c) predicted median displacements (50th percentile).

The proposed models are based on the assumption that the non-zero D are log-normally distributed. Fig. 8 shows the normalized Q-Q plots of the displacement residuals for the two models. The residuals generally match the 1:1 line, especially in the range of -2 to 2 , which justifies the choice of truncation value and the regression approaches.

Model Comparisons

In this section, the performance of the proposed models is compared with the BT07 model. An earthquake scenario with $M_w = 7$ that occurred on a strike-slip fault is considered. Permanent displacement analysis is performed for hypothetical slopes located at a soft soil site and a R_{rup} of 10 km. The ground-motion prediction equations proposed by Campbell and Bozorgnia (2014) and Travararou et al. (2003) are adopted to estimate PGA, S_a , and I_a , respectively.

The predicted distributions of slope displacements for three k_y cases using three predictive models (i.e., $[S_a(1.5T_s), I_a]$, $[PGA, S_a(2\text{ s})]$, and BT07) are shown in Fig. 9. The predicted median nonzero displacements and the probabilities of zero displacement with respect to T_s are plotted in Figs. 9(a and b), respectively. Fig. 9(c) shows the predicted median (50th percentile) displacements computed via Eq. (6) for $k_y = 0.05$, 0.1 , and $0.2g$, respectively. All these plots indicate a similar trend, except that the new model predictions tend to die down faster with an increasing T_s at $T_s > 1\text{ s}$. This difference might be due to the overestimation of the BT07 model at large T_s . As was reported in Bray

and Travararou (2007), the residuals of the BT07 model exhibited a negative bias for $T_s > 1$ s, indicating an overestimation of displacement.

Discussions

Two predictive models for seismic displacements are developed following the analytical framework of the BT07 model. Compared with the BT07 model, several distinguishing features are incorporated in the new models. First, a much expanded ground-motion database is used in this study. Second, both models developed use two IMs as predictor variables. Many studies have indicated the advantage of considering a vector IM on engineering applications (e.g., Saygili and Rathje 2008; Wang 2012). Furthermore, the average sliding displacements from two horizontal components of ground motions were used for the regression analysis in the BT07 model, while the horizontal components of each recording are regarded as separate empirical data in this study.

The developed models could be regarded as updates of the BT07 model. Specifically, the [PGA, $S_a(2\text{ s})$] model has some desirable features. First, the model does not need to incorporate an M_w term in the functional form, indicating that it satisfies the sufficiency requirement. Second, this model uses T_s -independent IMs as predictors, making it convenient to utilize existing PGA and $S_a(2\text{ s})$ hazard maps for a regional-scale slope displacement analysis (e.g., Du and Wang 2014). The application of the vector IM models requires the study of correlation between IMs, which has been extensively studied recently (e.g., Baker and Jayaram 2008; Wang and Du 2013; Du and Wang 2013; Huang and Wang 2015).

Conclusions

Two predictive models (i.e., [$S_a(1.5T_s), I_a$] and [PGA, $S_a(2\text{ s})$]) are developed for estimating the earthquake-induced slope displacements based on equivalent-linear fully coupled analysis and 3,714 ground-motion records selected from the NGA-West2 database. Both models use vector IMs as predictor variables, which provide better representation of ground-motion characteristics compared with a scalar IM model. The proposed models, together with existing ones, can be used in a logic-tree framework to quantify the epistemic uncertainty of seismic displacements in engineering applications.

Acknowledgments

This work was supported by Hong Kong Research Grants Council through General Research Fund No. 16213615 and DAG11EG03G. The authors thank the associate editor and two anonymous reviewers for their helpful comments.

Supplemental Data

Further information about the selection of predictor variables for regressing analysis, including Eqs. (S1) and (S2) and Figs. S1 and S2, is available online in the ASCE Library (www.ascelibrary.org).

References

Ancheta, T. D., et al. 2014. "NGA-West2 database." *Earthquake Spectra* 30 (3): 989–1005. <https://doi.org/10.1193/070913EQS197M>.

- Baker, J. W., and N. Jayaram. 2008. "Correlation of spectral acceleration values from NGA ground motion models." *Earthquake Spectra* 24 (1): 299–317. <https://doi.org/10.1193/1.2857544>.
- Bray, J. D., and T. Travararou. 2007. "Simplified procedure for estimating earthquake-induced deviatoric slope displacements." *J. Geotech. Geoenviron. Eng.* 133 (4): 381–392. [https://doi.org/10.1061/\(ASCE\)1090-0241\(2007\)133:4\(381\)](https://doi.org/10.1061/(ASCE)1090-0241(2007)133:4(381)).
- Campbell, K. W., and Y. Bozorgnia. 2014. "NGA-West2 ground motion model for the average horizontal components of PGA, PGV, and 5% damped linear acceleration response spectra." *Earthquake Spectra* 30 (3): 1087–1115. <https://doi.org/10.1193/062913EQS175M>.
- Darendeli, M. B. 2001. "Development of a new family of normalized modulus reduction and material damping curves." Ph.D. thesis, Dept. of Civil, Architectural and Environmental Engineering, Univ. of Texas at Austin.
- Du, W., and G. Wang. 2013. "Intra-event spatial correlations for cumulative absolute velocity, Arias intensity and spectral accelerations based on regional site conditions." *Bull. Seismol. Soc. Am.* 103 (2): 1117–1129. <https://doi.org/10.1785/0120120185>.
- Du, W., and G. Wang. 2014. "Fully probabilistic seismic displacement analysis of spatially distributed slopes using spatially correlated vector intensity measures." *Earthquake Eng. Struct. Dyn.* 43 (5): 661–679. <https://doi.org/10.1002/eqe.2365>.
- Du, W., and G. Wang. 2016. "A one-step Newmark displacement model for probabilistic seismic slope displacement hazard analysis." *Eng. Geol.* 205: 12–23. <https://doi.org/10.1016/j.enggeo.2016.02.011>.
- Huang, D., and G. Wang. 2015. "Region-specific spatial cross-correlation model for stochastic simulation of regionalized ground-motion time histories." *Bull. Seismol. Soc. Am.* 105 (1): 272–284. <https://doi.org/10.1785/0120140198>.
- Jibson, R. W. 2011. "Methods for assessing the stability of slopes during earthquakes—A retrospective." *Eng. Geol.* 122 (1): 43–50. <https://doi.org/10.1016/j.enggeo.2010.09.017>.
- Luco, N., and C. A. Cornell. 2007. "Structure-specific scalar intensity measures for near-source and ordinary earthquake ground motions." *Earthquake Spectra* 23 (2): 357–392. <https://doi.org/10.1193/1.2723158>.
- Macedo, J., J. Bray, and T. Travararou. 2017. "Simplified procedure for estimating seismic slope displacements in subduction zones." In *Proc., 16th World Conf. on Earthquake Engineering*, Santiago, Chile.
- Newmark, N. M. 1965. "Effects of earthquakes on dams and embankments." *Géotechnique* 15 (2): 139–160. <https://doi.org/10.1680/geot.1965.15.2.139>.
- Rathje, E. M., and J. D. Bray. 2000. "Nonlinear coupled seismic sliding analysis of earth structures." *J. Geotech. Geoenviron. Eng.* 126 (11): 1002–1014. [https://doi.org/10.1061/\(ASCE\)1090-0241\(2000\)126:11\(1002\)](https://doi.org/10.1061/(ASCE)1090-0241(2000)126:11(1002)).
- Rathje, E. M., Y. Wang, P. J. Stafford, G. Antonakos, and G. Saygili. 2014. "Probabilistic assessment of the seismic performance of earth slopes." *Bull. Earthquake Eng.* 12 (3): 1071–1090. <https://doi.org/10.1007/s10518-013-9485-9>.
- Saygili, G., and E. M. Rathje. 2008. "Empirical predictive models for earthquake-induced sliding displacements of slopes." *J. Geotech. Geoenviron. Eng.* 134 (6): 790–803. [https://doi.org/10.1061/\(ASCE\)1090-0241\(2008\)134:6\(790\)](https://doi.org/10.1061/(ASCE)1090-0241(2008)134:6(790)).
- Song, J., and A. Rodriguez-Marek. 2015. "Sliding displacement of flexible earth slopes subject to near-fault ground motions." *J. Geotech. Geoenviron. Eng.* 141 (3): 04014110. [https://doi.org/10.1061/\(ASCE\)GT.1943-5606.0001233](https://doi.org/10.1061/(ASCE)GT.1943-5606.0001233).
- Travararou, T., J. D. Bray, and N. A. Abrahamson. 2003. "Empirical attenuation relationship for Arias intensity." *Earthquake Eng. Struct. Dyn.* 32 (7): 1133–1155. <https://doi.org/10.1002/eqe.270>.
- Wang, G. 2012. "Efficiency of scalar and vector intensity measures for seismic slope displacements." *Front. Struct. Civ. Eng.* 6 (1): 44–52.
- Wang, G., and W. Du. 2013. "Spatial cross-correlation models for vector intensity measures (PGA, I_a , PGV, and SAs) considering regional site conditions." *Bull. Seismol. Soc. Am.* 103 (6): 3189–3204. <https://doi.org/10.1785/0120130061>.